PPPL-2479
UC20-F

PPPL-2479

MHD ACTIVITY AND ENERGY LOSS DURING BETA SATURATION AND COLLAPSE AT HIGH BETA POLOIDAL IN PBX

By

H.W. Kugel, S. Sesnic, K. Bol, M. Chance, H. Fishman, R. Fonck, G. Gammel, R. Kaita, S. Kaye, B. LeBlanc, J. Manickam, W. Morris, M. Okabayashi, S.F. Paul, M. Reusch, and H. Takahashi

OCTOBER 1987

PLASMA PHYSICS LABORATORY

PRINCETON UNIVERSITY
PRINCETON, NEW JERSEY

PREPARED FOR THE U.S. DEPARTMENT OF ENERGY,
UNDER CONTRACT DE-AC02-76-CHO-3073.

PPPL--2479

DE88 003453

MHD ACTIVITY AND ENERGY LOSS DURING BETA SATURATION AND COLLAPSE AT HIGH BETA POLOIDAL IN PBX

H.W. Kugel, S. Sesnic, K. Bol, M. Chance, H. Fishman, R. Fonck, G. Gammel, R. Kaita, S. Kaye, B. LeBlanc, J. Manickam, W. Morris,[a] M. Okabayashi, S.F. Paul, M. Reusch, and H. Takahashi

Plasma Physics Laboratory, Princeton University
Princeton, New Jersey 08544, USA

Abstract

High-β experiments, in medium to high-q tokamak plasmas, exhibit a temporal β saturation and collapse. This behavior has been attributed to ballooning, ideal kink, or tearing modes. In PBX, a unique diagnostic capability allowed studies of the relation between MHD and energy loss for neutral-beam-heated (< 6 MW), mildly indented (10-15%), nearly steady I_p discharges that approached the Troyon-Gruber limit. Under these conditions, correlations between MHD activity and energy losses have shown that the latter can be almost fully accounted for by various long wavelength MHD instabilities and that there is no need to invoke high-n ballooning modes in PBX.

(a) Permanent address: Balliol College, Oxford University, U.K.

1. Introduction.

One of the central issues in high-β experiments, in medium to high-q tokamak plasmas, is whether the observed temporal β saturation and collapse are caused by ballooning, ideal kink, or tearing modes. Several explanations have been proposed for the β-limits found for different tokamaks and experimental conditions. In ISX-B, for example, a deterioration in confinement at high-β (i.e., a soft β-limit) was observed, but this deterioration did not exhibit a correlation with the observed m=1/n=1 mode [1], and hence, ballooning modes were proposed as a possible cause for this β-limit [2]. In PBX, in low-q ($q \leq 3.5$), high current-ramp discharges [3], and in D-III [4], for certain limiter discharges, a disruptive β-limit attributed to the n=1 external kink mode was observed. In ASDEX [5] and PBX [6], very similar types of neutral-beam-heated discharges typically underwent transitions into the H-mode. After this transition, β rose initially, but then saturated and eventually "collapsed" at constant plasma current and heating power. In ASDEX, since edge relaxation phenomena (ERP) alone could not explain the additional energy losses during the saturation and collapse phases, and since no other observed MHD activity could be held responsible for the saturation and collapse, ballooning modes were invoked to explain this β-limit. In PBX, however, it was possible to correlate these additional energy losses with various observed MHD phenomena (i.e., sawteeth, fishbones, continuous mode, and ERP), and there was no need to postulate the existence of ballooning modes. The PBX investigations reported previously [6] were performed at medium q-edge (4 to 5) and β-poloidal (1 to 1.2) values. In this paper, we report the extension of β saturation and collapse studies to high q-edge (>6), high β-poloidal (>2) discharges. We will conclude that globally the high β-poloidal discharges generally behave similarly to those at lower β-poloidal reported previously [6], but that the detailed behavior of the MHD depends on β-poloidal.

2. Experimental Conditions and Results.

The plasma parameters in these high q-edge, high β-poloidal, H-mode discharges were as follows: I_p = 250 kA, B_t = 1.7 T, q-edge = 7, P_{inj} = 5 MW, plasma elongation =

1.3, a_{mid} = 37 cm, R = 152 cm, indentation = 5%, $\langle\beta_t\rangle$ = 1 to 1.5%, and the Troyon-Gruber scaling parameter $\beta_c = (\mu_o I_p / a_{mid} B_t)$ = 0.6 to 0.8.

In PBX, we were able to examine directly the relation between MHD activity and energy loss using a unique diamagnetic loop that was placed inside the vacuum chamber and which had a very short response time and high amplitude resolution. There was a very good correlation between the energy losses observed with the diamagnetic loop and the MHD events as observed in the X-ray diodes, Mirnov signals, neutron losses, charge exchange fast particle effluxes, and Hα emission. A typical discharge is shown in Fig. 1; shown are the displaced toroidal flux as measured by the diamagnetic loop and the Hα emission from the divertor. The first neutral beam was injected at 350 ms, with another following at 400 ms, and finally the last two beams were injected at 450 ms. All four beams were injected until 660 ms. Since the plasma current and shape were held constant during neutral beam injection, the displaced toroidal flux signal generally reflected the evolution of β-poloidal. The L-mode lasted until 485 ms, at which time the transition to the H-mode occurred. These discharges did not exhibit sawteeth, and the transition to the H-mode often appeared to be triggered by relatively strong fishbones. After the H-mode transition, the discharge exhibited three phases: β increase, saturation, and collapse.

a. β-Increase Phase. After the transition to the H-mode, over a period of 20 ms, the internal energy increased at a rate of 0.9 MW, and the confinement improved steadily except for the strong fishbone at 495 ms. There was little or no MHD activity during the period of increasing β except for this fishbone. During the last part of the β-increase phase, fishbones became more severe resulting in non-negligible loss of fast particles. This was the cause of the start of the β-saturation phase at 520 ms.

b. β-Saturation Phase. As shown in Figs. 1 and 2, the saturation period lasted for about 50 ms, ending at 570 ms. This period was characterized by three kinds of MHD activity, each with varying energy loss: fishbones, ERP, and a continuous mode. There were two types of fishbones, their difference being the modulation strength in various signals. The weaker fishbones were characterized by a weaker modulation of the X-ray signal, charge exchange fast particle effluxes, and Mirnov fluctuations, a smaller change in the modulation frequency, a smaller drop in diamagnetic signal, and an almost imperceptible and slow drop in neutron flux. The plasma energy loss was less than 0.4% and the neutron flux drop was less than 2%. The duration of the burst was also short, less than 0.5 ms. The frequency of the fishbone was typically between 20 and 30 kHz, dropping down to half of this frequency during the burst.

The stronger fishbones exhibited higher energy losses of up to 1.5%, larger neutron flux drops of up to 8%, and greater than a factor of two increase in the charge exchange efflux than for the weaker fishbones. The effect that most distinguished the stronger fishbones from the weaker ones was the effect on the X-ray radiation. The horizontal-viewing diodes indicated an out-in plasma column motion: the inner diodes showed an increase in signal, and the outer diodes a decrease. The vertical-viewing diodes showed only an increase in the signal, which intensified toward the edge of the plasma (up and down). The inferred plasma reconfiguration during the fishbone was very different from the sawtooth-like crash at lower q-edge and β-poloidal values. Here, the plasma appears to be pushed inward and further elongated.

The ERP often occurred 1 to 2 ms after any fishbone and always after a stronger fishbone.The ERP duration was normally a few hundred ms. A possible sequence of events is that the fishbone expels energy from the center, the energy propagates outward and builds up near the edge. After 1 to 2 ms, an ERP occurs, and energy is lost over a large region. This would imply that ERP may not be just an edge instability but may involve a large part of the minor radius. The ERP instability may be induced by high pressure, temperature, or current gradients that may have built up in response to the initial central energy expulsion. The energy loss due to the ERP was about 1%.

There was another type of the MHD activity, which was characteristic of only the β-saturation phase and was never observed during the β-collapse phase. This was an n=2 or n=3 mode as determined by the radial magnetic field coils with a higher unknown m number. This mode can be seen in the X-ray diode signals shown in Fig. 2 from 566 to 569.5 ms. The mode frequency was usually between 30 kHz (n=2) to 60 kHz ($n=3$) and the mode amplitude was saturated. This mode contributed very little to the additional energy losses, and was therefore not a strong participant in the β-saturation process.

The repetition time of the weaker fishbones was 1 to 2 ms, while that of the strong fishbones was about 5 ms. Using these repetition rates and the energy losses involved in each event, it is possible to account fully for the energy losses during the β-saturation, and thereby to ascribe the β-saturation effect to the three types of MHD behavior: weak fishbones, strong fishbones, and accompanying ERP. These additional energy losses are close to a total of 1 MW and are sufficient enough to cause the β-saturation.

c. β-Collapse Phase. The β-collapse phase usually began with the onset of a strong $n=1$ mode and was characterized by two types of MHD activity: a quasi-continuous $n=1$ mode and ERP. In Figs. 1 and 2 this phase starts at 570 ms and lasts until the end of the beam injection at 660 ms. Both the continuous mode and the ERP can be seen in Fig. 3.

At the beginning of the β-collapse phase, the amplitude of the continuous $n=1$ mode was modulated. A larger amplitude mode results in a stronger loss of fast particles, a larger drop in neutron flux, and a larger loss of plasma energy from the diamagnetic signal, thus establishing a correlation between the energy loss and the amplitude of the continuous mode. After the initial period, the mode amplitude saturated in the central part of the plasma column, but it continued to burst at the edge; the modulation is seen as a decrease in mode frequency and amplitude, and these decreases occurred at the time of each ERP. This modulation of the external part of the mode is well correlated with the change in the fast particle efflux, and the decay in the neutron flux and plasma energy. Using the correlation of this mode with the diamagnetic loop signal, the increase in modulation of the fast particle losses, and the drop in neutron flux, we can conclude that this mode is responsible for both the thermal and beam energy loss.

In Fig. 4, we compare this continuous mode at high β-poloidal and high q-edge with the mode at medium β-poloidal and medium q-edge for two typical discharges. The relative modulation and the phase of these two modes is shown as a function of the vertical position in the plasma. Although there are differences in the details of the phase structure of these modes, they both show a gradual, continuous phase shift across the central part of the plasma. They both have a phase change of approximately 180° between z=-20 and +20 cm. The large difference is in vertical distribution of the relative amplitude modulation. The medium β-poloidal and medium-q case (#255) shows a strong odd mode (possibly m=1) with radial coupling to strong higher m-number modes, whereas in the case of high β-poloidal and high-q (#5214), the radial coupling is stronger and there is no one dominant internal mode.

The ERP events as shown in Fig. 3 correlate well with sudden drops in the diamagnetic signal, with H_α spikes, with the drops in the external X-ray diodes, with the high frequency bursts (100 kHz and higher) in the radial field signal, and with the decrease in the fast particle loss modulation. They do not correlate at all with the drops in the neutron flux, indicating that the ERP losses represent only thermal energy losses. The ERP contribute 0.5% energy loss per event with a repetition time of 1.4 ms.

If we assume that the underlying plasma confinement properties during the β-collapse phase are the same as those at 500 msec when little or no MHD activity was present, we can determine what additional losses are ascribable to the MHD activity during the β-collapse. With this assumption, the dW/dt term at 580 ms should have a value of +1.1 MW. The total additional loss required to explain the β-collapse is 1.4 MW. An increase in radiated power, as measured by bolometry, accounts for 450 kW of this loss. The ERP contribute 400 kW to the loss, leaving 550 kW attributable to the n=1 continuous mode, thus making this mode contribute a comparable amount to the β-collapse.

3. Conclusions.

We have shown that the observed β-saturation and collapse in PBX can be explained in terms of long wavelength MHD and ERP activity, and that there is no need to invoke ballooning modes. The β-saturation and collapse phases are different in terms of the MHD activity. The saturation phase is dominated by the fishbones, ERP, and n=2 or n=3 modes, but only the fishbones and ERP contribute substantially to the energy loss. The β-collapse is caused primarily by a strong n=1 continuous mode, and to a lesser extent ERP, and additional radiation losses. The n=1 continuous mode is responsible for both thermal and beam energy losses, and the ERP only for thermal energy losses. This continuous mode for high β-poloidal differs from the one observed at medium β-poloidal by not having an m=1 component, and by exhibiting a strong radial coupling of modes and no one dominant internal mode.

Acknowledgments

We wish to acknowledge the contributions of P. Couture, W. Heidbrink, K. Ida, K. Jaehnig, G. Jahns, G. Navratil, N. Ohyabu, D. Ward, and the PBX Engineering and Technical Staff. This work supported by the U.S. DoE Contract No. DE-AC02-76-CHO-3073.

References

1. J.L.Dunlop *et al.*, Phys. Rev. Lett. 48, 538 (1982).

2. M. Murakami *et al.*, in Plasma Physics and Controlled Nuclear Fusion Research (Proc. 10th Inter. Conf., London, 1984) Vol. I (IAEA, Vienna, 1985) 87.

3. K. Bol *et al.*, Phys. Rev. Lett. 57, 1891 (1986).

4. R.D. Stambaugh *et al.*, in Plasma Physics and Controlled Nuclear Fusion Research (Proc. 10th Inter. Conf., London, 1984) Vol. I (IAEA, Vienna, 1985) 217.

5. O. Gruber *et al.*, in Proc. of 11th Inter. Conf. on Plasma Phys. and Contr. Nuclear Fusion Research, Kyoto, 1986 (IAEA, Vienna, 1987).

6. M. Okabayashi *et al.*, in Proc. of 11th Inter. Conf. on Plasma Phys. and Contr. Nuclear Fusion Research, Kyoto, 1986 (IAEA, Vienna, 1987).

Figure Captions

Fig. 1. Diamagnetic loop and $H\alpha$ signals from the divertor region during neutral beam injection.

Fig. 2. Signals from various diagnostics during the last part of β-saturation.

Fig. 3. Signals from different diagnostics during a part of the β-collapse phase.

Fig. 4. Comparison of the amplitude modulation and the phase change of the $n=1$ continuous mode during the β-collapse phase for medium q-edge medium-β (#255), and for high q-edge high β-poloidal (#5214).

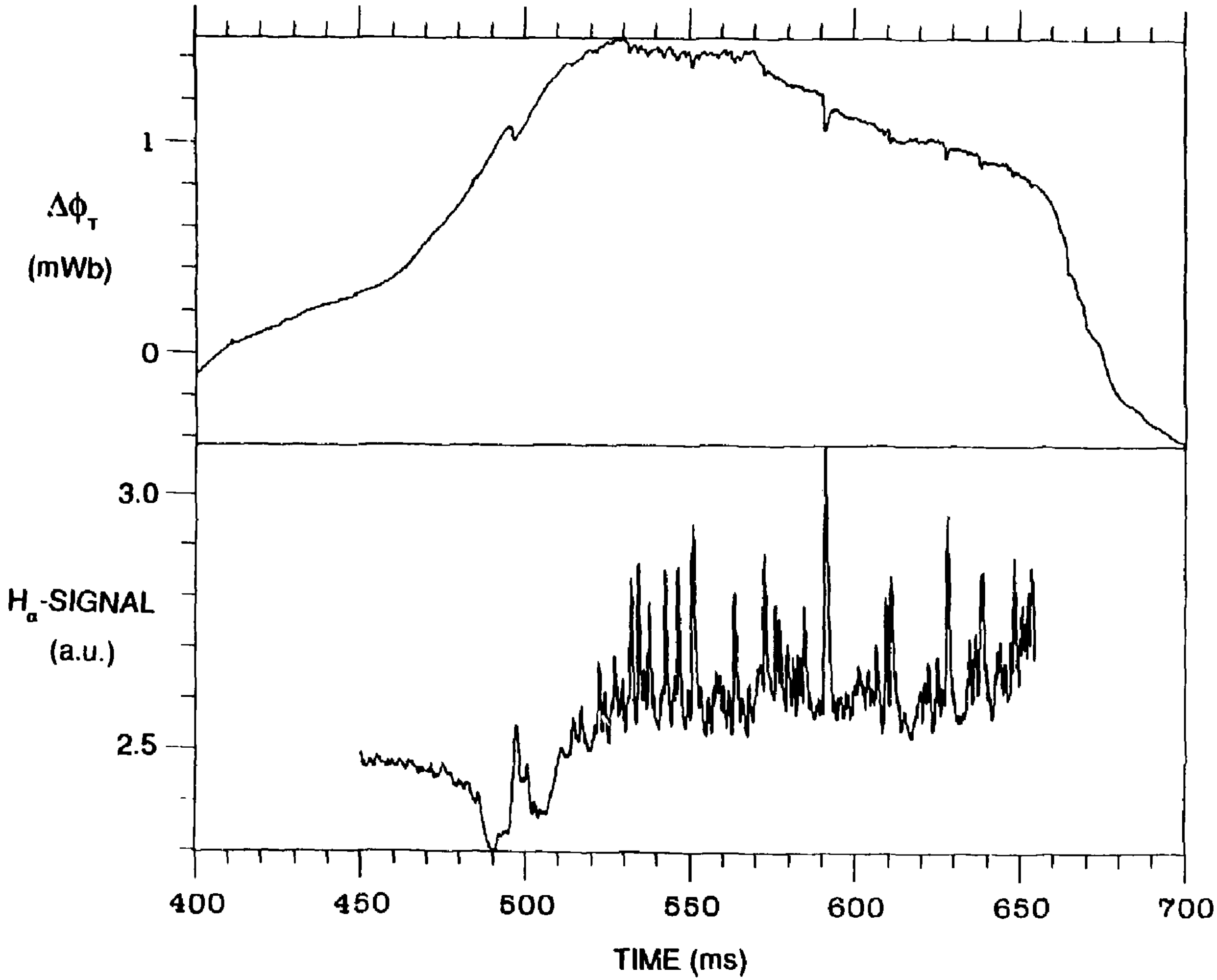

$\Delta\phi_T$ (mWb)
1
0
H_α-SIGNAL (a.u.)
3.0
2.5
400
450
500
550
600
650
700
TIME (ms)

Fig. 1

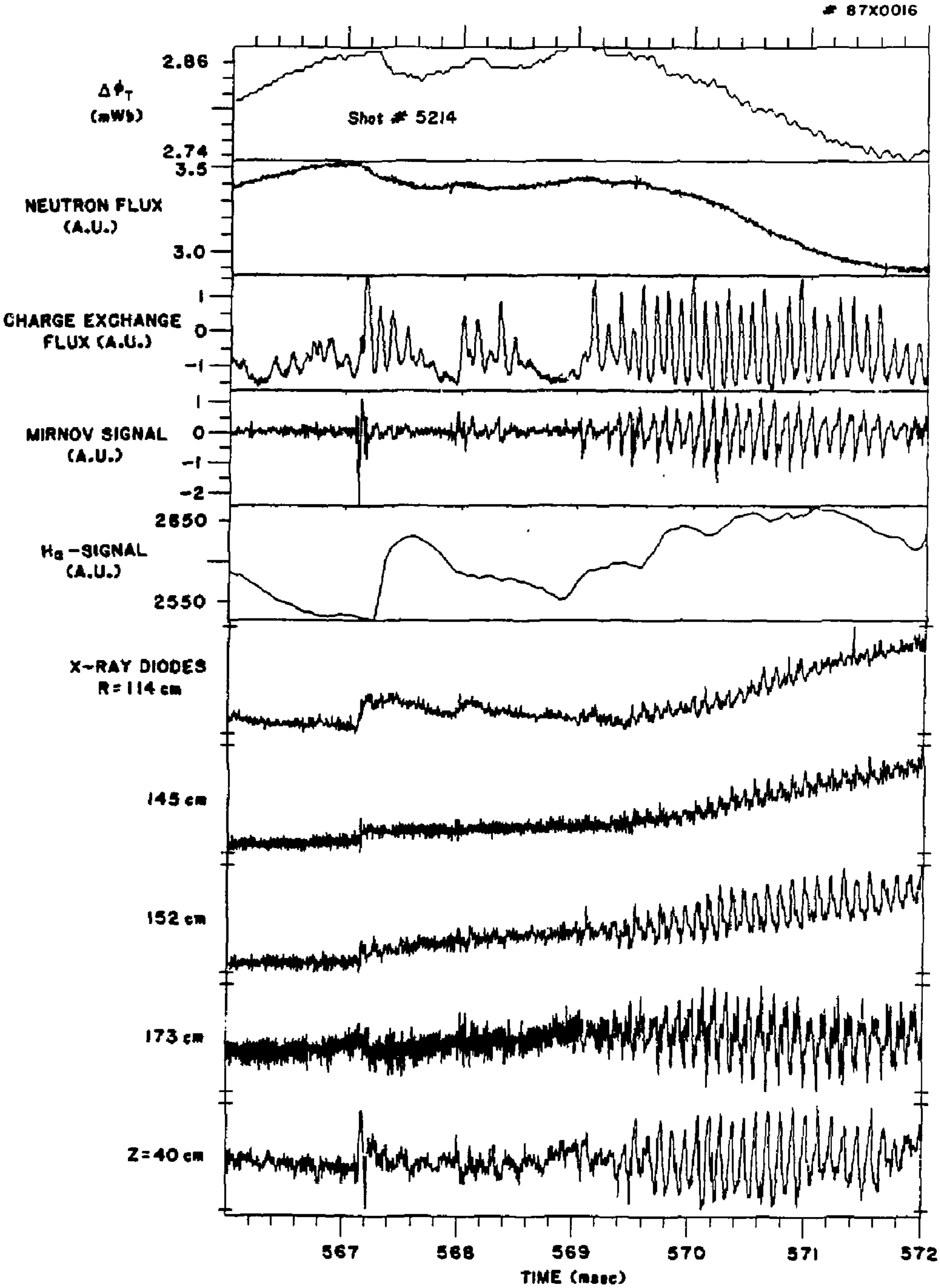

87X0016
Shot # 5214
2.86
Δφ_T
(mWb)
2.74
3.5
NEUTRON FLUX
(A.U.)
3.0
CHARGE EXCHANGE
FLUX (A.U.)
1
0
-1
MIRNOV SIGNAL
(A.U.)
-2
2650
Hα-SIGNAL
(A.U.)
2550
X-RAY DIODES
R=114 cm
145 cm
152 cm
173 cm
Z=40 cm
567
568
569
570
571
572
TIME (msec)

Fig. 2

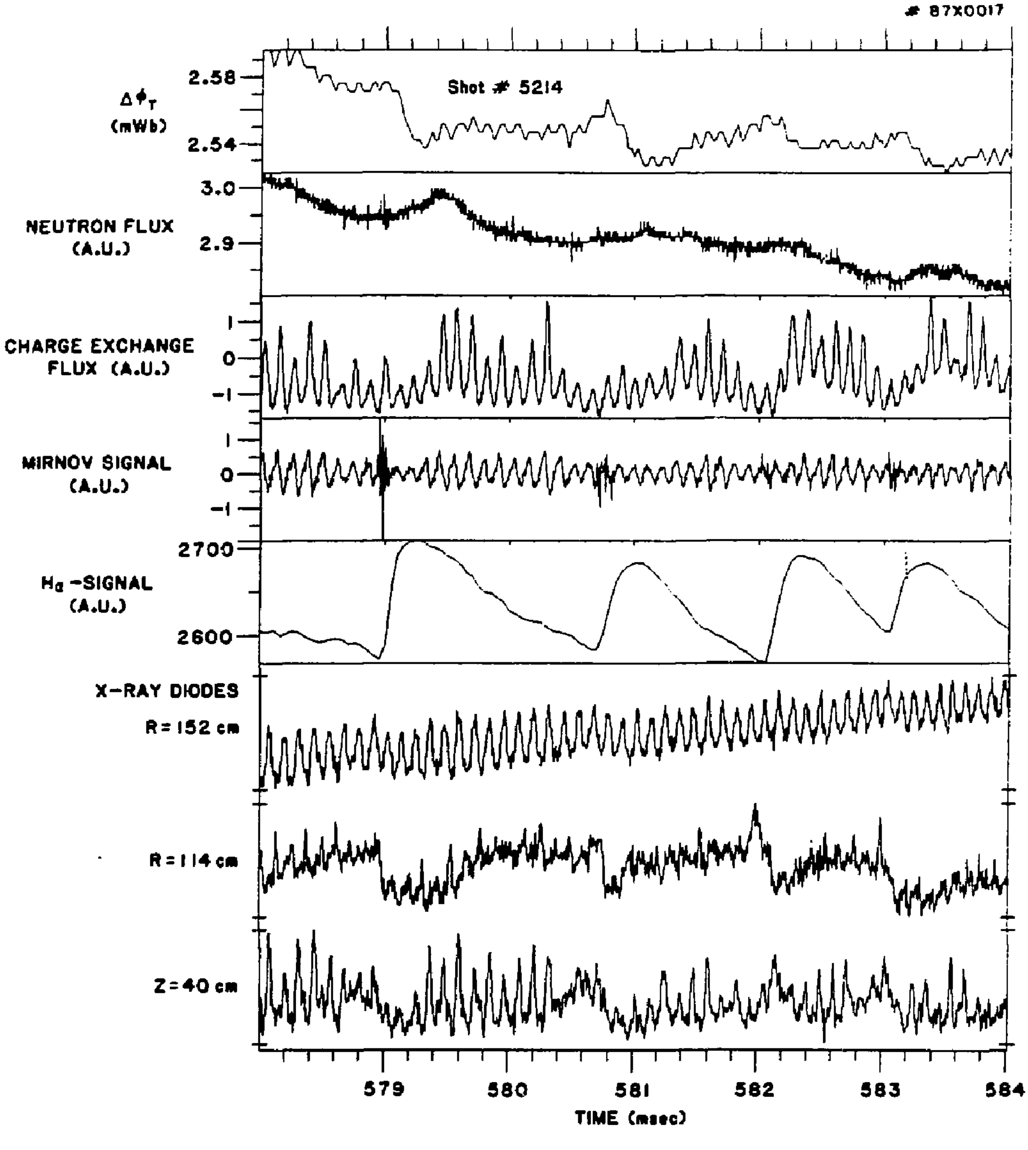

87X0017
Shot # 5214
$\Delta\phi_T$ (mWb)
2.58
2.54
NEUTRON FLUX (A.U.)
3.0
2.9
CHARGE EXCHANGE FLUX (A.U.)
1
0
−1
MIRNOV SIGNAL (A.U.)
1
0
−1
H_α −SIGNAL (A.U.)
2700
2600
X−RAY DIODES
R = 152 cm
R = 114 cm
Z = 40 cm
579
580
581
582
583
584
TIME (msec)

Fig. 3

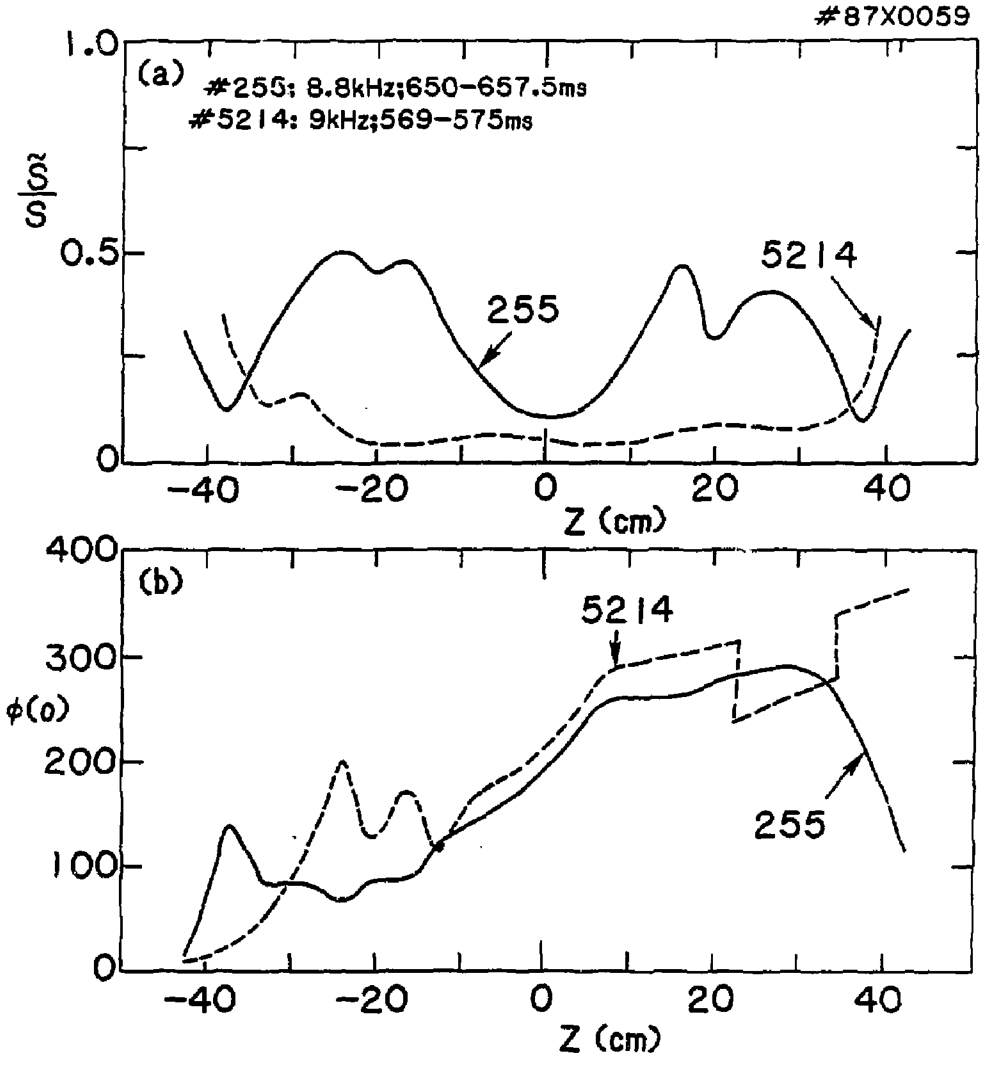
#87X0059
(a)
#255: 8.8kHz;650-657.5ms
#5214: 9kHz;569-575ms
1.0
0.5
0
5214
255
-40
-20
0
20
40
Z (cm)
400
(b)
300
200
100
0
5214
255
-40
-20
0
20
40
Z (cm)

Fig. 4

EXTERNAL DISTRIBUTION IN ADDITION TO UC-20

Dr. Frank J. Paoloni, Univ of Wollongong, AUSTRALIA
Prof. M.H. Brennan, Univ Sydney, AUSTRALIA
Plasma Research Lab., Australian Nat. Univ., AUSTRALIA
Prof. I.R. Jones, Flinders Univ., AUSTRALIA
Prof. F. Cap, Inst Theo Phys, AUSTRIA
Prof. M. Heindler, Institut fur Theoretische Physik, AUSTRIA
M. Goossens, Astronomisch Instituut, BELGIUM
Ecole Royale Militaire, Lab de Phys Plasmas, BELGIUM
Com. of European, Dg XII Fusion Prog, BELGIUM
Prof. R. Boucique, Laboratorium voor Natuurkunde, BELGIUM
Dr. P.H. Sakanaka, Univ Estadual, BRAZIL
Instituto De Pesquisas Espaciasi-INPE, BRAZIL
Library, Atomic Energy of Canada Limited, CANADA
Dr. M.P. Bachynski, MPB Technologies, Inc., CANADA
Dr. H.M. Skarsgard, Univ of Saskatchewan, CANADA
Dr. H. Barnard, University of British Columbia, CANADA
Prof. J. Teichmann, Univ. of Montreal, CANADA
Prof. S.R. Sreenivasan, University of Calgary, CANADA
Prof. Tudor W. Johnston, INRS-Energie, CANADA
Dr. C.R. James, Univ. of Alberta, CANADA
Dr. Peter Lukac, Komenskeho Univ, CZECHOSLOVAKIA
The Librarian, Culham Laboratory, ENGLAND
Mrs. S.A. Hutchinson, JET Library, ENGLAND
C. Mouttet, Lab. de Physique des Milieux Ionisés, FRANCE
J. Radet, CEN/CADARACHE - Bat 506, FRANCE
Dr. Tom Mual, Academy Bibliographic, HONG KONG
Preprint Library, Cent Res Inst Phys, HUNGARY
Dr. B. Dasgupta, Saha Inst, INDIA
Dr. R.K. Chhajlani, Vikram Univ. INDIA
Dr. P. Kaw, Institute for Plasma Research, INDIA
Dr. Phillip Rosenau, Israel Inst Tech, ISRAEL
Prof. S. Cuperman, Tel Aviv University, ISRAEL
Librarian, Int'l Ctr Theo Phys, ITALY
Prof. G. Rostagni, Univ Di Padova, ITALY
Miss Clelia De Palo, Assoc EURATOM-ENEA, ITALY
Biblioteca, del CNR EURATOM, ITALY
Dr. H. Yamato, Toshiba Res & Dev, JAPAN
Prof. I. Kawakami, Atomic Energy Res. Institute, JAPAN
Prof. Kyoji Nishikawa, Univ of Hiroshima, JAPAN
Direc. Dept. Lg. Tokamak Res. JAERI, JAPAN
Prof. Satoshi Itoh, Kyushu University, JAPAN
Research Info Center, Nagoya University, JAPAN
Prof. S. Tanaka, Kyoto University, JAPAN
Library, Kyoto University, JAPAN
Prof. Nobuyuki Inoue, University of Tokyo, JAPAN
S. Mori, JAERI, JAPAN
M.H. Kim, Korea Advanced Energy Research Institute, KOREA
Prof. D.I. Choi, Adv. Inst Sci & Tech, KOREA
Prof. B.S. Liley, University of Waikato, NEW ZEALAND
Institute of Plasma Physics, PEOPLE'S REPUBLIC OF CHINA
Librarian, Institute of Phys., PEOPLE'S REPUBLIC OF CHINA
Library, Tsing Hua University, PEOPLE'S REPUBLIC OF CHINA
Z. Li, Southwest Inst. Physics, PEOPLE'S REPUBLIC OF CHINA
Prof. J.A.C. Cabral, Inst Superior Tecn, PORTUGAL
Dr. Octavian Petrus, AL I CUZA University, ROMANIA
Dr. Johan de Villiers, Plasma Physics, AEC, SO AFRICA
Prof. M.A. Hellberg, University of Natal, SO AFRICA
Fusion Div. Library, JEN, SPAIN
Dr. Lennart Stenflo, University of UMEA, SWEDEN
Library, Royal Inst Tech, SWEDEN
Prof. Hans Wilhelmson, Chalmers Univ Tech, SWEDEN
Centre Phys des Plasmas, Ecole Polytech Fed, SWITZERLAND
Bibliotheek, Fom-Inst Voor Plasma-Fysica, THE NETHERLANDS
Dr. D.D. Ryutov, Siberian Acad Sci, USSR
Dr. G.A. Eliseev, Kurchatov Institute, USSR
Dr. V.A. Glukhikh, Inst Electro-Physical, USSR
Dr. V.T. Tolok, Inst. Phys. Tech. USSR
Dr. L.M. Kovrizhnykh, Institute Gen. Physics, USSR
Prof. T.J.M. Boyd, Univ College N Wales, WALES
Nuclear Res. Establishment, Julich Ltd., W. GERMANY
Bibliothek, Inst. Fur Plasmaforschung, W. GERMANY
Dr. K. Schindler, Ruhr Universität, W. GERMANY
ASDEX Reading Rm, IPP/Max-Planck-Institut fur Plasmaphysik, W. GERMANY
Librarian, Max-Planck Institut, W. GERMANY
Prof. R.K. Janev, Inst Phys, YUGOSLAVIA